

1
2
3 **Supporting Information for:**
4

5 **A cardiolipin-deficient mutant of *Rhodobacter sphaeroides* has an altered cell**
6 **shape and is impaired in biofilm formation**
7

8
9 Ti-Yu Lin¹, Thiago M. A. Santos¹, Wayne S. Kontur^{2,3}, Timothy J. Donohue^{2,3},
10 Douglas B. Weibel^{1,4,5*}
11

12
13 ¹ *Department of Biochemistry, University of Wisconsin–Madison, Madison, Wisconsin,*
14 *USA*

15 ² *Department of Bacteriology, University of Wisconsin–Madison, Madison, Wisconsin, USA*

16 ³ *DOE Great Lakes Bioenergy Research Center, Madison, Wisconsin, USA*

17 ⁴ *Department of Chemistry, University of Wisconsin–Madison, Madison, Wisconsin, USA*

18 ⁵ *Department of Biomedical Engineering, University of Wisconsin–Madison, Madison,*
19 *Wisconsin, USA*
20

21 * Author to whom correspondence should be addressed:

22 Douglas B. Weibel

23 Department of Biochemistry

24 6424 Biochemical Sciences Building

25 440 Henry Mall

26 Phone: +1 (608) 890-1342

27 Fax: +1 (608) 265-0764

28 E-mail: weibel@biochem.wisc.edu
29

30 *Running title:* Cardiolipin affects cell shape and biofilm formation
31

32 *Keywords:* cardiolipin | *Rhodobacter sphaeroides* | cell shape | biofilms
33
34
35
36
37
38
39
40
41
42
43
44

45 **Results**

46 ***RSP_0113* does not encode a cardiolipin synthase in *Rhodobacter sphaeroides***

47 To investigate the origins of the residual 10% of the cardiolipin (CL) in the CL3
48 mutant, we performed a BLAST search and found another candidate *CL synthase (cls)*
49 gene in *R. sphaeroides*: *RSP_0113* (GenBank entry YP_353188) (1, 2). *RSP_0113* is 25%
50 identical and 41% similar to the amino acid sequence of *Escherichia coli* CL synthase,
51 and contains a phospholipase D domain that is a characteristic motif found in CL
52 synthases. We cloned the *RSP_0113* gene into an *E. coli* expression plasmid pTrc99A
53 and an *R. sphaeroides* expression plasmid pIND4, and expressed it in the *E. coli*
54 CL-deficient mutant BKT12 (3) and *R. sphaeroides* CL3, respectively. We were unable
55 to detect CL in phospholipids extracted from BKT12 cells harboring a
56 plasmid-encoded *RSP_0113* gene or nor were we able to detect increased CL in
57 analogous CL3 transformants (data not shown) by thin-layer chromatogram. These
58 results suggest that *RSP_0113* is not a CL synthase in either bacterium and leave us
59 uncertain of the origins of the residual 10% CL in *R. sphaeroides* CL3.

60

61

62

63

64

65

66

67 **Materials and Methods**

68 **Confocal scanning laser microscopy of biofilms**

69 Stationary phase cell cultures were standardized to an absorbance of 1.0 (λ , 600 nm).

70 The standardized cultures were inoculated 1/100 in Sistrom's succinate medium

71 containing 5 $\mu\text{g}/\text{ml}$ Nile Red in a chamber slide with hydrophobic plastic surfaces

72 (ibidi, Verona, WI) and incubated for 72 h at 30°C. After washed with water to

73 remove planktonic cells, biofilms were imaged on a Nikon A1R- Si confocal

74 microscope. Images were processed with NIS-Elements AR software.

75

76

77

78

79

80

81

82

83

84

85

86

87

88

89 **References**

- 90 1. **Altschul SF, Madden TL, Schaffer AA, Zhang J, Zhang Z, Miller W, Lipman**
91 **DJ.** 1997. Gapped BLAST and PSI-BLAST: a new generation of protein
92 database search programs. *Nucleic Acids Res* **25**:3389-3402.
- 93 2. **Kontur WS, Schackwitz WS, Ivanova N, Martin J, Labutti K, Deshpande S,**
94 **Tice HN, Pennacchio C, Sodergren E, Weinstock GM, Noguera DR,**
95 **Donohue TJ.** 2012. Revised sequence and annotation of the *Rhodobacter*
96 *sphaeroides* 2.4.1 genome. *J Bacteriol* **194**:7016-7017.
- 97 3. **Tan BK, Bogdanov M, Zhao J, Dowhan W, Raetz CR, Guan Z.** 2012.
98 Discovery of a cardiolipin synthase utilizing phosphatidylethanolamine and
99 phosphatidylglycerol as substrates. *Proc Natl Acad Sci U S A* **109**:16504-16509.

100

101

102

103

104

105

106

107

108

109

110

111 **Figures and Legends**

112 **Figure S1. Nile Red does not change cell shape and impede cell growth of *R.***

113 *sphaeroides*. (A) Images depicting the morphology of *R. sphaeroides* wild-type (WT)
114 and CL3 cells grown aerobically in Sistrof's succinate medium containing 5 µg/mL
115 Nile Red at 30°C with shaking at 200 rpm. Each data point was determined by
116 imaging 300 cells using phase contrast brightfield microscopy and using ImageJ to
117 determine cell width and length. The values represent mean values ± standard
118 deviations. Differences of the cell shape parameters between the two strains were
119 analyzed by Student's *t test*. The P value for all parameters measured was < 0.001.
120 Scale bar, 2 µm. (B) Growth curves of *R. sphaeroides* WT and CL3 cells grown with
121 shaking in glass test tubes at 30°C in Sistrof's succinate medium containing 5
122 µg/mL Nile Red. The values represent mean values ± standard deviations obtained
123 from three independent experiments. Although a ~0.1 difference in absorbance (λ ,
124 600 nm) was observed at stationary phase, colony-forming units (CFUs) of the WT
125 and CL3 strains were not significantly different (WT: 1.6×10^9 CFU/mL, CL3: $1.5 \times$
126 10^9 CFU/mL).

127

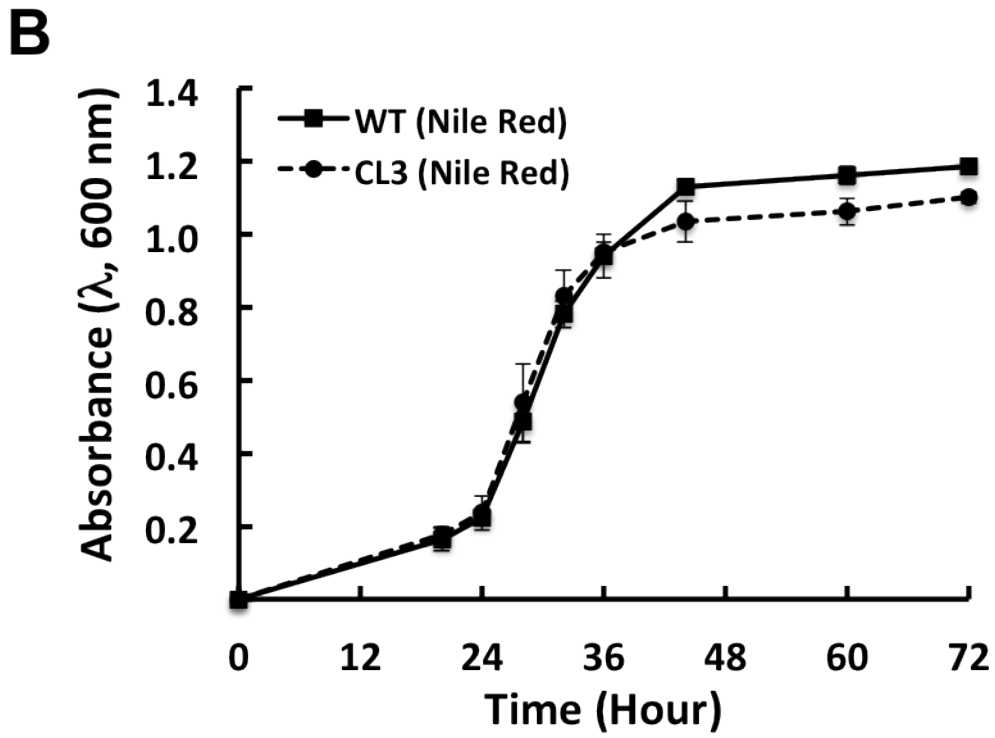
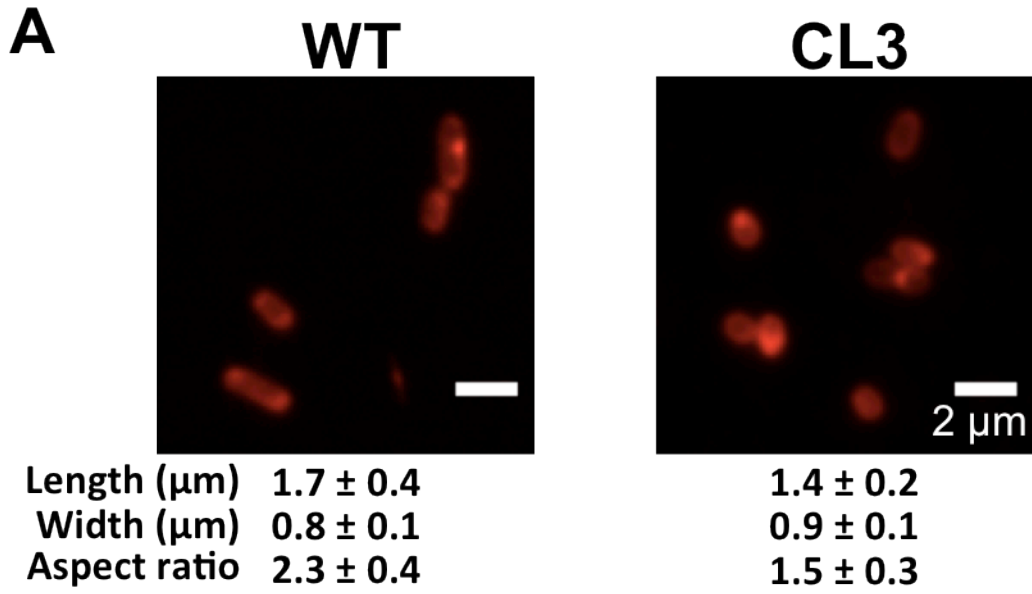
128

129

130

131

132



133

134 Figure S1

135

136

137

138

139 **Figure S2. Confocal laser scanning micrographs of *R. sphaeroides* WT and CL3**
140 **biofilms.** *R. sphaeroides* WT and CL3 biofilms were grown on a chamber slide with
141 hydrophobic plastic surfaces for 72 h at 30°C in Siström's succinate medium
142 containing 5 µg/ml Nile Red and imaged using a confocal microscope. Upper panels:
143 orthogonal views. Scale bar, 10 µm. Lower panels: 3-D reconstructions of confocal
144 microscopy images. The thickness of *R. sphaeroides* WT biofilms was 20 µm. In
145 contrast, the CL3 strain formed biofilms that were typically ~9-µm thick.

146

147

148

149

150

151

152

153

154

155

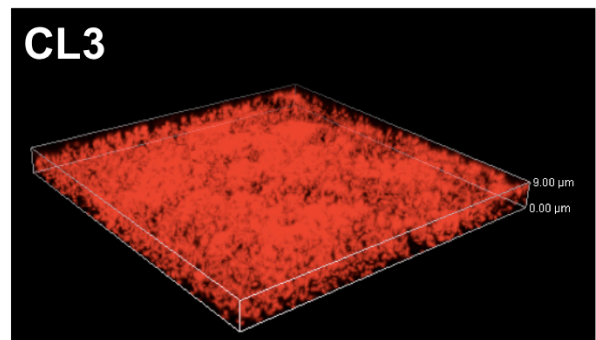
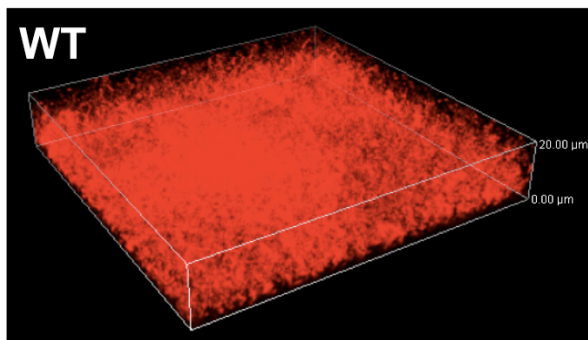
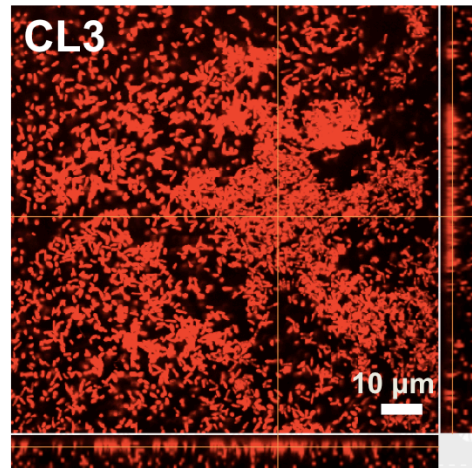
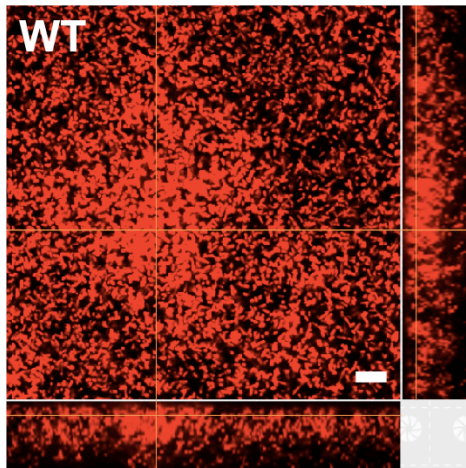
156

157

158

159

160



161

162 **Figure S2**

163

164

165

166

167

168

169

170

171

172

173

174 **Figure S3.** Representative micrographs of *R. sphaeroides* WT and CL3 cells attached
175 to surfaces. *R. sphaeroides* WT and CL3 cells were grown on a chamber slide with
176 hydrophobic plastic surfaces at 30°C in Siström's succinate medium. Cells attached
177 to the surface were imaged at 1 h after inoculation. Images were acquired using
178 phase contrast brightfield microscopy. Scale bar, 2 μm.

179

180

181

182

183

184

185

186

187

188

189

190

191

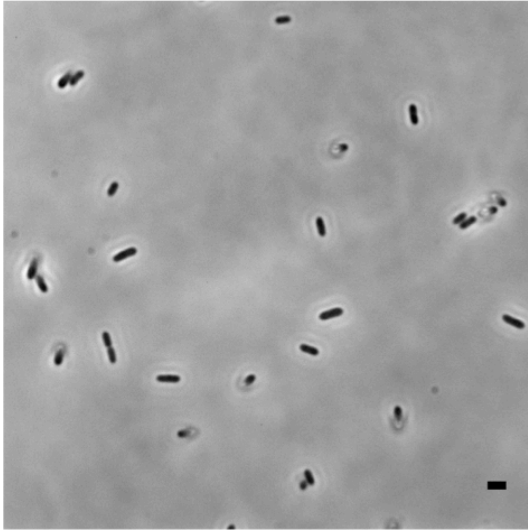
192

193

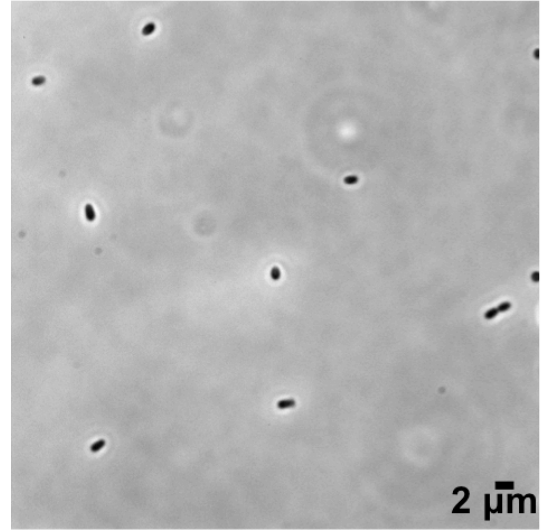
194

195

WT



CL3



196

197 **Figure S3**

198

199

200

201

202

203

204

205

206

207

208

209

210

211

212 **Figure S4. Quantification of *R. sphaeroides* WT and CL3 biofilms grown in wells**
213 **of a glass bottom microtiter plate.** Biofilms were grown on a glass bottom microtiter
214 plate (MatTek, Ashland, MA) for 72 h at 30°C in Siström's succinate medium,
215 followed by staining with crystal violet (CV). The extent of biofilm formation was
216 determined by the absorbance of CV at λ , 550 nm. The values represent mean values
217 \pm standard deviations obtained from three independent experiments, each
218 performed in 8 replicates. *R. sphaeroides* strain CL3 displayed a 50% reduction in
219 biofilm formation compared with the WT strain after 72 h of incubation.

220

221

222

223

224

225

226

227

228

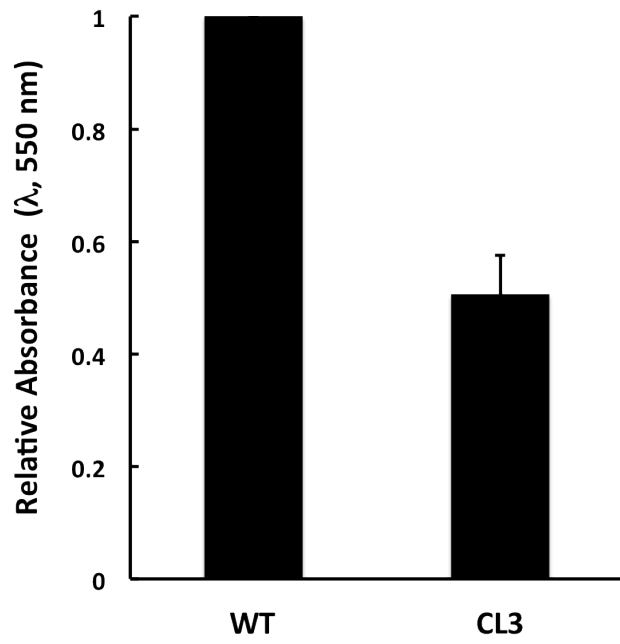
229

230

231

232

233



234

235 **Figure S4**

236

237

238

239

240

241

242

243

244

245

246

247

248

249 **Figure S5. Exopolysaccharides (EPS) extracted from planktonic cultures of *R.***
250 ***sphaeroides* WT and CL3 cells.** Cells were grown with shaking in glass test tubes for
251 72 h at 30°C in Siström's succinate medium. The EPS in growth media was
252 precipitated by adding absolute ethanol to a final concentration of 75%, separated on
253 an SDS-polyacrylamide gel using electrophoresis, and visualized by silver staining.
254 EPS from both *R. sphaeroides* strains displayed similar banding patterns and was
255 present in similar amounts.

256

257

258

259

260

261

262

263

264

265

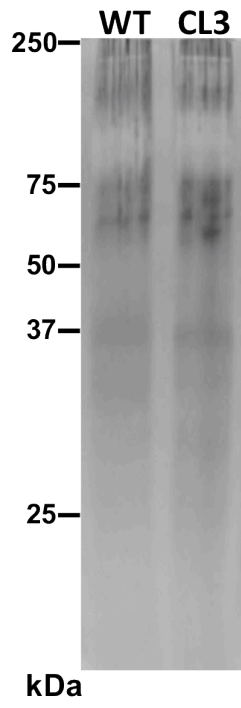
266

267

268

269

270



271

kDa

272 Figure S5